The P granule component PGL-1 promotes the localization and silencing activity of the PUF protein FBF-2 in germline stem cells

Ekaterina Voronina, Alexandre Paix and Geraldine Seydoux*

SUMMARY

In the *C. elegans* germline, maintenance of undifferentiated stem cells depends on the PUF family RNA-binding proteins FBF-1 and FBF-2. FBF-1 and FBF-2 are 89% identical and are required redundantly to silence the expression of mRNAs that promote meiosis. Here we show that, despite their extensive sequence similarity, FBF-1 and FBF-2 have different effects on target mRNAs. FBF-1 promotes the degradation and/or transport of meiotic mRNAs out of the stem cell region, whereas FBF-2 prevents translation. FBF-2 activity depends on the P granule component PGL-1. PGL-1 is required to localize FBF-2 to perinuclear P granules and for efficient binding of FBF-2 to its mRNA targets. We conclude that multiple regulatory mechanisms converge on meiotic RNAs to ensure silencing in germline stem cells. Our findings also support the view that P granules facilitate mRNA silencing by providing an environment in which translational repressors can encounter their mRNA targets immediately upon exit from the nucleus.

KEY WORDS: Germline stem cells, RNA silencing, P granules, PUF domain, PGL-1, *Caenorhabditis elegans*

INTRODUCTION

Post-transcriptional control of gene expression is common in the germline, where protein expression patterns are often determined by RNA-binding proteins that bind to sequences in the 3′ UTR (reviewed by Rangan et al., 2008; Kimble, 2011; Voronina et al., 2011). Germ cells contain a unique type of RNA granule, or 'nuage', that localizes to the cytoplasmic face of the nuclear envelope. In *Drosophila*, *C. elegans* and zebrafish, the nuage has been implicated in the biogenesis of small RNAs, as several components of the RNAi machinery, including Argonautes, localize there (reviewed by Voronina et al., 2011). Studies in *C. elegans* have revealed that the nuage ('P granules') overlay clusters of nuclear pores and are the primary sites of mRNA export from the nucleus, raising the possibility that P granules also regulate mRNAs (Pitt et al., 2000; Sheth et al., 2010). Core components of the P granules include two classes of RNA-binding proteins: the VASA-related RNA helicases GLH-1, GLH-2 and GLH-4 and the RGG domain proteins PGL-1 and PGL-3 (reviewed by Updike and Strome, 2010). In this study, we investigate a connection between PGL-1 and mRNA regulation in germline stem cells.

In adult hermaphrodites, germ cells are arranged in a distal-to-proximal order of differentiation in two U-shaped tubes connected to a common uterus (reviewed by Hubbard and Greenstein, 2005). The distal end of each tube contains ~250 cells that divide by mitosis (mitotic zone). The cells are connected to a common cytoplasmic core (rachis) and are displaced proximally each time a cell divides (Fig. 1A). Cells at the distalmost tip include the stem cells, which continue to divide by mitosis indefinitely into adulthood. Cells in the proximal half of the mitotic zone are considered a transient-amplifying population: they continue to divide by mitosis but begin to accumulate low levels of meiotic proteins (Hansen et al., 2004; Cinquin et al., 2010). Meiotic protein expression peaks in the transition zone, where cells initiate chromosome pairing in preparation for recombination in the pachytene region (Fig. 1A).

Maintenance of mitotically dividing cells in the mitotic zone requires FBF-1 and FBF-2, two 89% identical PUF domain RNA-binding proteins (Crittenden et al., 2002). Immunoprecipitation experiments suggest that FBF-1 and FBF-2 bind thousands of mRNAs, including several meiotic mRNAs that are transcribed but silenced in the mitotic zone (Kershner and Kimble, 2010; Merritt and Seydoux, 2010). In the 3′ UTR of meiotic mRNAs, FBF-1 and FBF-2 recognize a motif (UCnUGUnnnAU) required for silencing in the mitotic zone (Bernstein et al., 2005; Merritt and Seydoux, 2010; Qiu et al., 2012). In the absence of both FBF-1 and FBF-2, all cells in the mitotic zone express meiotic proteins precociously, enter meiosis and differentiate into sperm (Crittenden et al., 2002). *fbf-1 fbf-2* hermaphrodites do not make oocytes and are sterile. *fbf-1* and *fbf-2* single mutants are fertile but have smaller (*fbf-1*) or larger (*fbf-2*) mitotic zones, suggesting that, although redundant for fertility, FBF-1 and FBF-2 also have unique roles (Lamont et al., 2004). Here, we provide further evidence that FBF-1 and FBF-2 have distinct activities and demonstrate a requirement for PGL-1 in FBF-2-dependent mRNA silencing.

MATERIALS AND METHODS
Nematode culture and RNAi
C. elegans strains (supplementary material Table S1) were derived from Bristol N2 and cultured according to standard protocols (Brenner, 1974) at 20°C or 25°C as indicated.

RNAi treatments were performed by feeding L4 hermaphrodites bacteria expressing double-stranded RNA for 24 hours. F1 progeny were transferred to fresh RNAi plates and examined as adults. The following RNAi constructs were used: *glh-4*, *pgl-3* (Kamath and Ahringer, 2003) and *glh-1*, *pgl-1* (genomic fragments covering full coding sequence) cloned in pL4440 (Timmons and Fire, 1998).

Howard Hughes Medical Institute, Department of Molecular Biology and Genetics, Johns Hopkins University School of Medicine, Baltimore, MD 21205, USA.

*Author for correspondence (gseydoux@jhmi.edu)

Generation of transgenic worms

FBF-1 (Merritt et al., 2008) and FBF-2 (this study) transgenes were constructed by Gateway cloning (Invitrogen) using the *pie-1* promoter and *fbf-1* or *fbf-2* genomic coding and 3′ UTR sequences, and introduced into worms by microparticle bombardment (Praitis et al., 2001). GFP::FBF-1 rescues the sterility of the *fbf-1 fbf-2* double mutant (Lee et al., 2007). GFP::FBF-2 rescues the expanded mitotic region of the *fbf-2(q738)* mutant, but not the shortened region of *fbf-1(ok91)* (data not shown).

In situ hybridization

In situ hybridizations were performed as described previously (Raj et al., 2008), with the following variations: dissected *C. elegans* gonads were fixed in –20°C methanol and stored at –20°C. Fixed samples were rehydrated in 1:1 PBS with 0.1% Tween 20 (PBS-Tw):methanol, washed five times with PBS-Tw, post-fixed for 1 hour at room temperature in 4% paraformaldehyde in PBS and washed three times with PBS-Tw and twice with 2× SSC. Quasar570 dye-labeled oligonucleotide probes were purchased from Biosearch Technologies and hybridized as described (Raj et al., 2008). Gonads were washed once with PBS-Tw and three times with PBS before mounting. In transgenic animals expressing GFP fusion proteins, residual GFP fluorescence was detectable following the in situ hybridization protocol.

Antibody generation and western blots

Polyclonal rabbit antiserum PA2388 was generated against the FBF-1 peptide EEGNLRLMRTFSP and affinity purified by Open Biosystems (Huntsville, AL, USA). For immunoblotting, the following primary antibodies were used: rabbit PA2388 anti-FBF-1 at 1:20 (26 µg/ml); mouse monoclonal anti-GFP JL-8 (Clontech) at 1:240; mouse monoclonal anti-tubulin DM1A (Sigma-Aldrich) at 1:1000; and mouse monoclonal anti-PGL-1/PGL-3 KT3 [Developmental Studies Hybridoma Bank (DSHB), University of Iowa] at 1:10. Secondary reagents were ECL Plex Cy5-conjugated goat anti-rabbit or goat anti-mouse antibodies (GE Healthcare/Amersham) at 1:2500 or HRP-Protein A (BD Biosciences) at 1:1000. Blots reacted with fluorescent secondary antibodies were scanned in a Typhoon 9410 imager (GE Healthcare) and quantified using ImageJ (NIH). Blots reacted with HRP-conjugated secondary reagents were developed using HyGlo Quick Spray Reagent (Denville).

To assess the specificity of the anti-FBF-1 antibody, extracts were prepared from synchronized cultures of *C. elegans* young adults that were either wild type or single mutants for *fbf-1(ok91)*, *fbf-2(q738)* or *pgl-1(ct131)* by repeated freeze-thaw in 1× NuPage LDS sample buffer (Invitrogen) containing 200 mM DTT, followed by sonication and heating for 10 minutes at 70°C. Lysates were separated on 7% SDS-PAGE gels (Invitrogen) and proteins were transferred to Immobilon-P membrane (Millipore). After blocking in TBS/Tween (50 mM Tris-HCl, pH 7.5, 0.18 M NaCl, 0.06% Tween 20) with 5% non-fat dry milk, the blots were probed with the indicated dilutions of antibodies in blocking solution. For comparing the amounts of GFP::FBF-2 protein in wild-type and *fbf-1(ok91)* backgrounds, the lysates of appropriate transgenic strains were prepared and treated as above. For analyzing the results of immunoprecipitations, aliquots of immunoprecipitation eluates were mixed with LDS sample buffer and DTT and analyzed as above.

Immunolocalization and microscopy

Adult hermaphrodites were washed in PBS and germlines were dissected on poly-L-lysine-treated slides, covered with a coverslip to ensure attachment to the slide surface, and flash-frozen on aluminium blocks chilled on dry ice. The samples were fixed for 1 minute in 100% methanol (–20°C) followed by 5 minutes in 2% EM grade paraformaldehyde in 100 mM K_2HPO_4 pH 7.2 at room temperature. The samples were blocked for at least 30 minutes in PBS containing 0.1% BSA and 0.1% Tween 20 (PBTw). Primary antibodies were diluted in PBTw as follows: rabbit anti-FBF-1 PA2388 1:150; rabbit anti-FBF-2 (Lamont et al., 2004) 1:5; mouse anti-PGL-1 (K76, DSHB) 1:12; mouse anti-PGL-1 (OIC1D4, DSHB) 1:10; chicken anti-GLH-2 (Gruidl et al., 1996) 1:300; chicken anti-GFP (Invitrogen) 1:200; rabbit anti-HTP-1/2 (Martinez-Perez et al., 2008) 1:200. Secondary antibodies were goat anti-rabbit IgG, anti-mouse IgG or IgM, and anti-chicken IgG conjugated to Alexa 488, Alexa 568 (Invitrogen) or Cy3 (Jackson ImmunoResearch) at 1:200. All primary antibody incubations were overnight at 4°C; all secondary antibody incubations were for 2 hours at room temperature. Confocal images were acquired with a Cascade QuantEM 512SC camera (Photometrics) attached to a Zeiss AxioImager with Yokogawa spinning disk confocal scanner and Slidebook software (Intelligent Imaging Innovations). Deconvolution of confocal stacks was performed with Slidebook using the calculated point-spread function and iterative algorithm. Image quantification was performed in Slidebook or ImageJ and image processing in Adobe Photoshop CS4. Correlation coefficients between the intensity of the *gld-1* mRNA in situ hybridization signal and GFP::H2B::*gld-1* 3′ UTR were determined for two germlines per genotype using GraphPad Prism software.

Immunoprecipitation and quantitative RT-PCR

GFP fusion proteins were immunoprecipitated from extracts of young adult worms with anti-GFP antibody (Roche) and bound RNA was eluted with 100 mM glycine pH 2.5 as described (Voronina and Seydoux, 2010). Before RNA isolation, an aliquot was removed from each eluate to quantify the target protein by quantitative western blotting. The relative amount of precipitated protein was used to normalize the amount of cDNA template used in the quantitative (q) PCR reaction. Total RNA was isolated from immunoprecipitates using Trizol (Invitrogen) and treated with DNase to remove DNA contamination (TURBO DNA-free, Ambion). cDNA was prepared from whole RNA samples using the iScript cDNA Synthesis Kit (Bio-Rad) using a mix of oligo(dT) and random primers. Real-time PCR reactions were performed in triplicate using adjusted cDNA volumes to account for differences in the amount of precipitated target protein. Primers for *gld-1*, *htp-1*, *htp-2*, *him-3* and *syp-3* were as described (Merritt and Seydoux, 2010). Primers for *tbb-2* and *ama-1* were designed to span exon-exon boundaries to avoid amplification of any residual genomic DNA. Enrichment of target mRNAs in each immunoprecipitate was calculated using ΔCt of anti-GFP and non-specific IgG samples and normalized for the enrichment of the non-specific control (*tbb-2*, set to 1.0) separately for each independent biological replicate. Following normalization, the enrichment values were combined to determine the average enrichment and differences between wild-type and *pgl-1* samples were evaluated for significance by paired *t*-test.

RESULTS

FBF-1 and FBF-2 exhibit different subcellular localizations

We characterized the distribution of FBF-1 and FBF-2 in fixed adult gonads using two complementary sets of reagents: polyclonal antibodies against FBF-1 (see Materials and methods) and FBF-2 (Lamont et al., 2004) to detect endogenous proteins, and anti-GFP antibody to detect GFP::FBF-1 and GFP::FBF-2 fusions in transgenic animals. Both approaches yielded the same results. As reported previously (Lamont et al., 2004), we detected FBF-1 and FBF-2 in the distal arm of the germline (Fig. 1B; supplementary material Fig. S1A). FBF-1 levels were uniformly high throughout the mitotic zone (supplementary material Fig. S1A); by contrast, FBF-2 levels were low in the first four to six rows and increased by 5-fold in subsequent rows (Fig. 1C,E; supplementary material Fig. S1A). FBF-1 and FBF-2 also differed in their subcellular distributions: FBF-1 localized to numerous cytoplasmic and perinuclear foci, whereas FBF-2 localized primarily to perinuclear foci and was more diffusely distributed in the cytoplasm (Fig. 1B).

To determine whether the FBF-1 and/or FBF-2 perinuclear foci correspond to P granules, we co-stained GFP::FBF-1 and GFP::FBF-2 with K76, an antibody against the P granule component PGL-1 (Kawasaki et al., 1998), and used deconvolution microscopy to evaluate colocalization in single confocal slices (Fig. 2; supplementary material Fig. S2E; Materials and methods). The majority (74%) of perinuclear GFP::FBF-1 foci did not overlap with P granules, although many (39%) were immediately adjacent
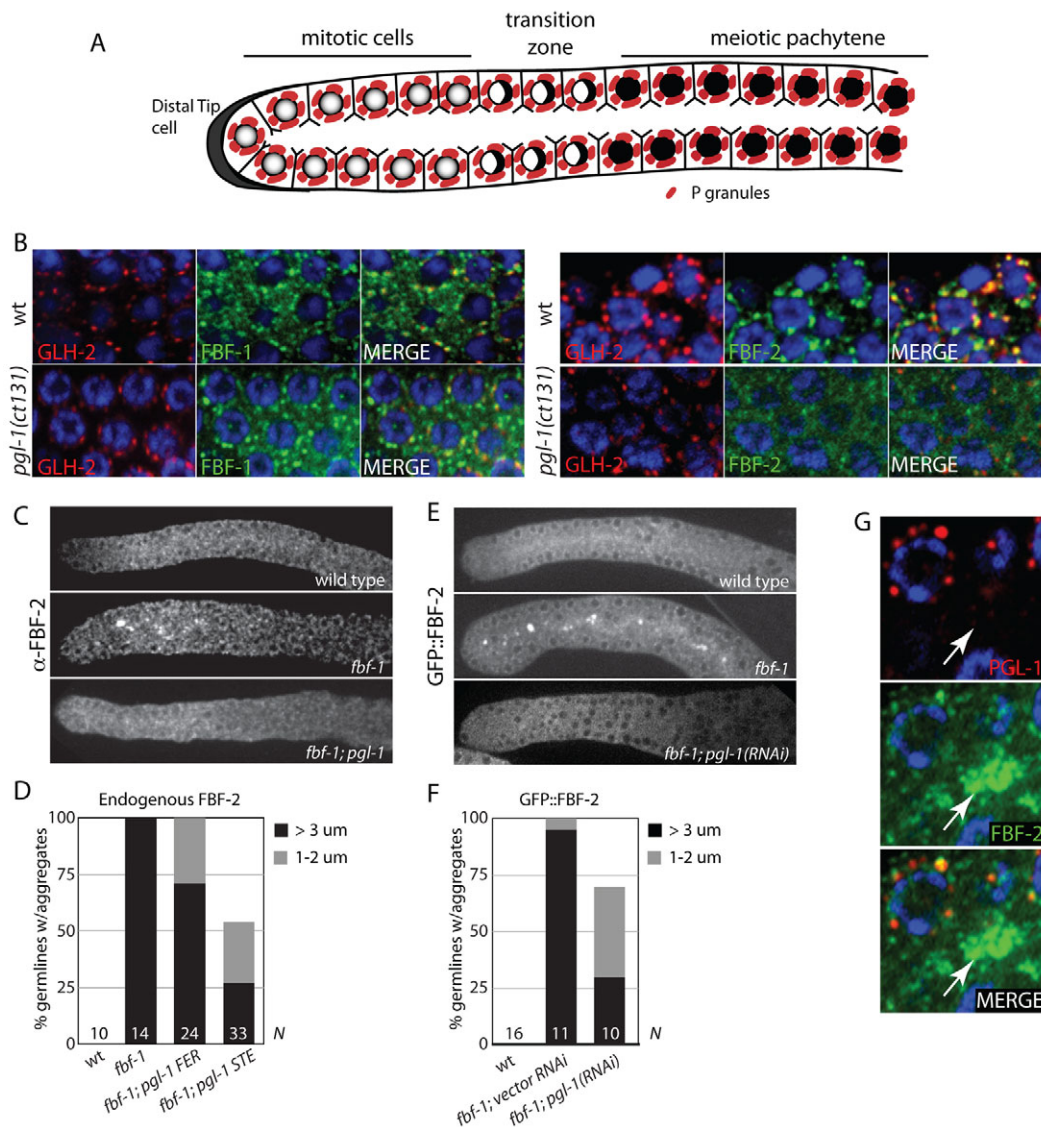
Fig. 1. FBF-1 and FBF-2 have distinct distributions in the distal gonad. (A) Diagram of the distal end of one gonadal arm. The gonad is a syncytium: each nucleus (circle) is surrounded by P granules (red) and partially enclosed by membranes open to a central cytoplasmic core (rachis). Signaling from the distal tip cell maintains cells at the distal end of the gonad in mitosis. In the transition zone, cells enter meiosis and initiate pairing of homologous chromosomes ('crescent' chromatin morphology). **(B)** Magnified view of the mitotic zone of wild-type and *pgl-1(ct131)* gonads double immunostained for the P granule component GLH-2 and FBF-1 or FBF-2. DNA is in blue. **(C,E)** Gonads of the indicated genotypes stained for FBF-2 or imaged live for GFP::FBF-2. FBF-2 localizes to aggregates in the mitotic zone of *fbf-1* mutant gonads. Formation of the aggregates depends on *pgl-1*. **(D,F)** The percentage of germlines with FBF-2 or GFP::FBF-2 aggregates in the indicated genotypes. *N*, number of hermaphrodites scored. **(G)** Magnified view of the distal region of an *fbf-1* mutant gonad co-stained for PGL-1 (OIC1D4 antibody) and FBF-2. The FBF-2 aggregate (arrow) is negative for PGL-1.

to a P granule (Fig. 2C). By contrast, 72% of GFP::FBF-2 perinuclear foci overlapped either completely or partially with P granules (Fig. 2B,C). Similar results were obtained comparing the distribution of endogenous FBF-1 with PGL-1 (Fig. 2A) and of the P granule component GLH-2 with endogenous FBF-1 or GFP::FBF-2 (supplementary material Fig. S2C,D). Double staining of FBF-1 and GFP::FBF-2 confirmed that FBF-1 and FBF-2 perinuclear foci are distinct, although they overlap occasionally (supplementary material Fig. S2A). We conclude that FBF-1 localizes to both cytoplasmic and perinuclear foci, the majority of which do not coincide with P granules. By contrast, FBF-2 localizes primarily to perinuclear foci that overlap with P granules and on occasion overlap with FBF-1 foci.

FBF-1 and FBF-2 have been reported to negatively regulate each other's abundance (Lamont et al., 2004). Consistent with those findings, FBF-1 levels were 2-fold higher in *fbf-2* mutants by western blot analysis and 1.6-fold higher by immunostaining (supplementary material Fig. S1B,D). GFP::FBF-2 levels were also higher in *fbf-1* mutants, but the increase was more modest when measured by western blot (1.5-fold; supplementary material Fig. S1C) and not significant when measured by immunostaining with an antibody to endogenous FBF-2 (supplementary material Fig. S1E). We noticed, however, that the distribution of FBF-2 and GFP::FBF-2 changed in *fbf-1* mutants: FBF-2 and GFP::FBF-2 localized to several large (over 1 μm) aggregates in the central core (rachis) of the mitotic zone of *fbf-1* mutants (Fig. 1C,E). These
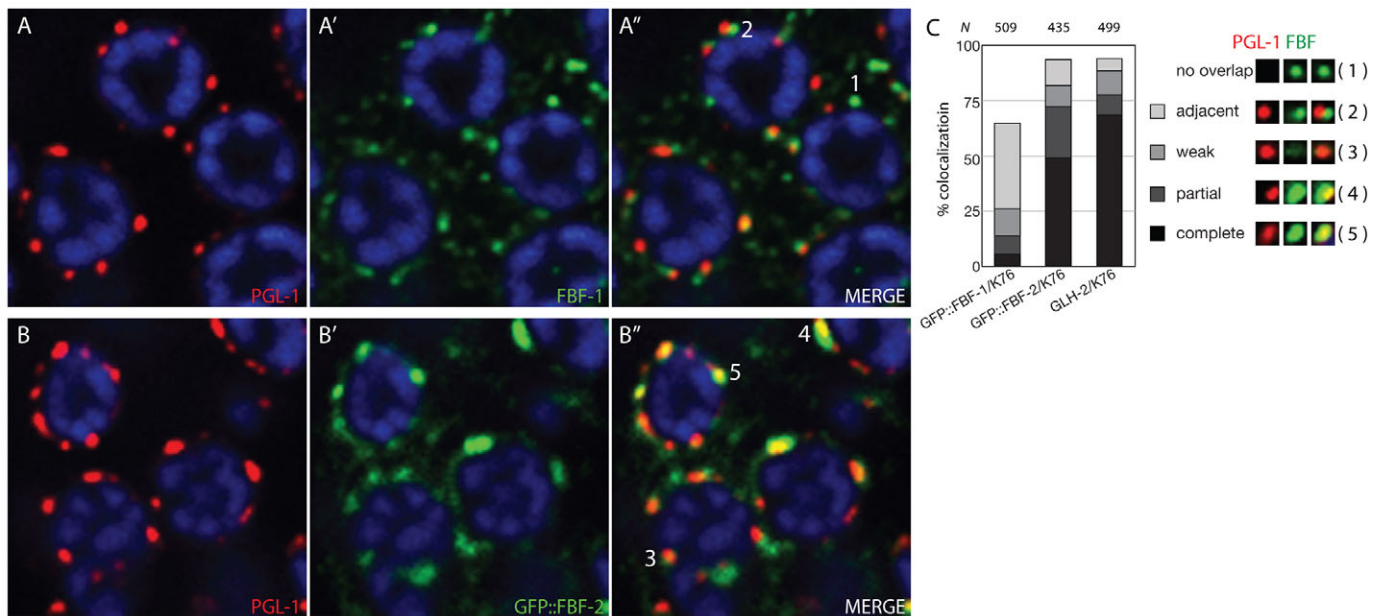
Fig. 2. FBF-1 and FBF-2 localize to distinct perinuclear granules. (**A**,**B**) Deconvolved optical sections of wild-type mitotic zone nuclei (blue) co-stained for PGL-1 (red; K76 antibody) and FBF-1 or GFP::FBF-2 (green). Numbers refer to examples of different overlap patterns as shown in C. (**C**) Percentage granule colocalization as determined from three GFP::FBF-1 and five GFP::FBF-2 gonadal sections imaged as in A and B. Five gonadal sections co-stained with GLH-2 and PGL-1 (K76 antibody; supplementary material Fig. S2B) were quantified for colocalization as controls. Only FBF-1 and GFP::FBF-2 granules immediately adjacent to nuclei ('perinuclear') were counted.

aggregates were specific to FBF-2: the P granule components GLH-2 and PGL-1 did not localize to FBF-2 aggregates in *fbf-1* mutants (Fig. 1G), and no FBF-1 aggregates were observed in *fbf-2* mutants (supplementary material Fig. S1A).

PGL-1 is required for FBF-2 localization to P granules

To determine whether the subcellular localization of FBF-1 and FBF-2 depends on P granule components, we characterized FBF-1 and FBF-2 distributions in *pgl-1(ct131)* mutants raised at the permissive temperature (20°C). At this temperature, *pgl-1(ct131)* mutants are fertile and have a small but distinct mitotic zone (Kawasaki et al., 1998) (supplementary material Fig. S3). We found that FBF-1 still localized to numerous foci in *pgl-1* mutants (Fig. 1B). By contrast, FBF-2 became more diffusely distributed in *pgl-1* mutants and no longer colocalized with P granules (detected with an antibody against GLH-2; Fig. 1B). We also observed that FBF-2 formed fewer aggregates in the rachis of *fbf-1;pgl-1* double mutants (Fig. 1C-F).

GLH-1 is a P granule component required to recruit PGL-1 to P granules (Spike et al., 2008a). We found that GFP::FBF-2 (but not GFP::FBF-1) was delocalized in *glh-1(RNAi)* gonads (supplementary material Fig. S1F). By contrast, no localization defects were detected in *glh-4(RNAi)* and *pgl-3(RNAi)* gonads, which maintain PGL-1 on P granules (supplementary material Fig. S1F). We conclude that P granule-localized PGL-1 is required to localize FBF-2 to P granules. PGL-1 also contributes to FBF-2 localization to aggregates in *fbf-1* mutants.

PGL-1 is required for FBF-2 function

fbf-1 fbf-2 double mutants are 100% sterile (Crittenden et al., 2002). We noticed that 41% of *fbf-1;pgl-1* hermaphrodites were also sterile (Fig. 3A). By contrast, only 5% of *fbf-2;pgl-1* worms were sterile (see supplementary material Table S1 for full

genotypes). Like *fbf-1 fbf-2* double mutants, sterile *fbf-1;pgl-1* hermaphrodites produce excess sperm and no oocytes (Fig. 3B), in contrast to wild-type worms, which produce both sperm and oocytes (Fig. 3C). These observations suggested that *pgl-1* might be required for *fbf-2* activity. If so, *fbf-1;pgl-1* double mutants should show the same range of phenotypes as *fbf-1 fbf-2* mutants.

To test this prediction, we first examined the expression patterns of meiotic proteins that are silenced by FBF-1 and FBF-2 in the mitotic zone. *fog-1* is a direct target of FBF-1 and FBF-2: the *fog-1* 3′ UTR contains FBF binding sites that silence FOG-1 protein expression in the mitotic region (Thompson et al., 2005). Expression of a GFP::H2B::*fog-1* 3′ UTR reporter is inhibited in the mitotic zone of wild-type, *fbf-1*, *fbf-2* and *pgl-1* single-mutant gonads, but is derepressed in *fbf-1 fbf-2* double-mutant gonads (Merritt et al., 2008) (supplementary material Fig. S3A). We observed ectopic expression of the *fog-1* 3′ UTR reporter in the mitotic region of 26% of fertile *fbf-1;pgl-1* double mutants and 55% of sterile *fbf-1;pgl-1* double mutants (Fig. 3D,E). We also observed derepression of the *fog-1* 3′ UTR reporter in 39% of *fbf-1;glh-1(RNAi)* gonads (supplementary material Fig. S3C).

HTP-1 and 2 are two highly homologous synaptonemal complex proteins that are silenced in the mitotic region redundantly by FBF-1 and FBF-2 (Merritt and Seydoux, 2010). We observed ectopic expression of HTP-1/2 in 18% of fertile *fbf-1;pgl-1* double mutants and in 53% of sterile *fbf-1;pgl-1* double mutants (Fig. 3F,G). In *fbf-1 fbf-2* mutants, ectopic HTP-1/2 in the mitotic zone accumulate in aggregates, which persist in pachytene germ cells and interfere with normal HTP-1/2 loading on paired chromosomes (Merritt and Seydoux, 2010). We observed similar aggregates and incomplete chromosome loading in *fbf-1;pgl-1* mutants (Fig. 3H). *fbf-1 fbf-2* mutants produce defective gametes with achiasmatic chromosomes (Thompson et al., 2005) leading to embryonic lethality (Luitjens et al., 2000). Similarly, we observed achiasmatic chromosomes in 70% of oocytes produced by fertile *fbf-1;pgl-1* hermaphrodites
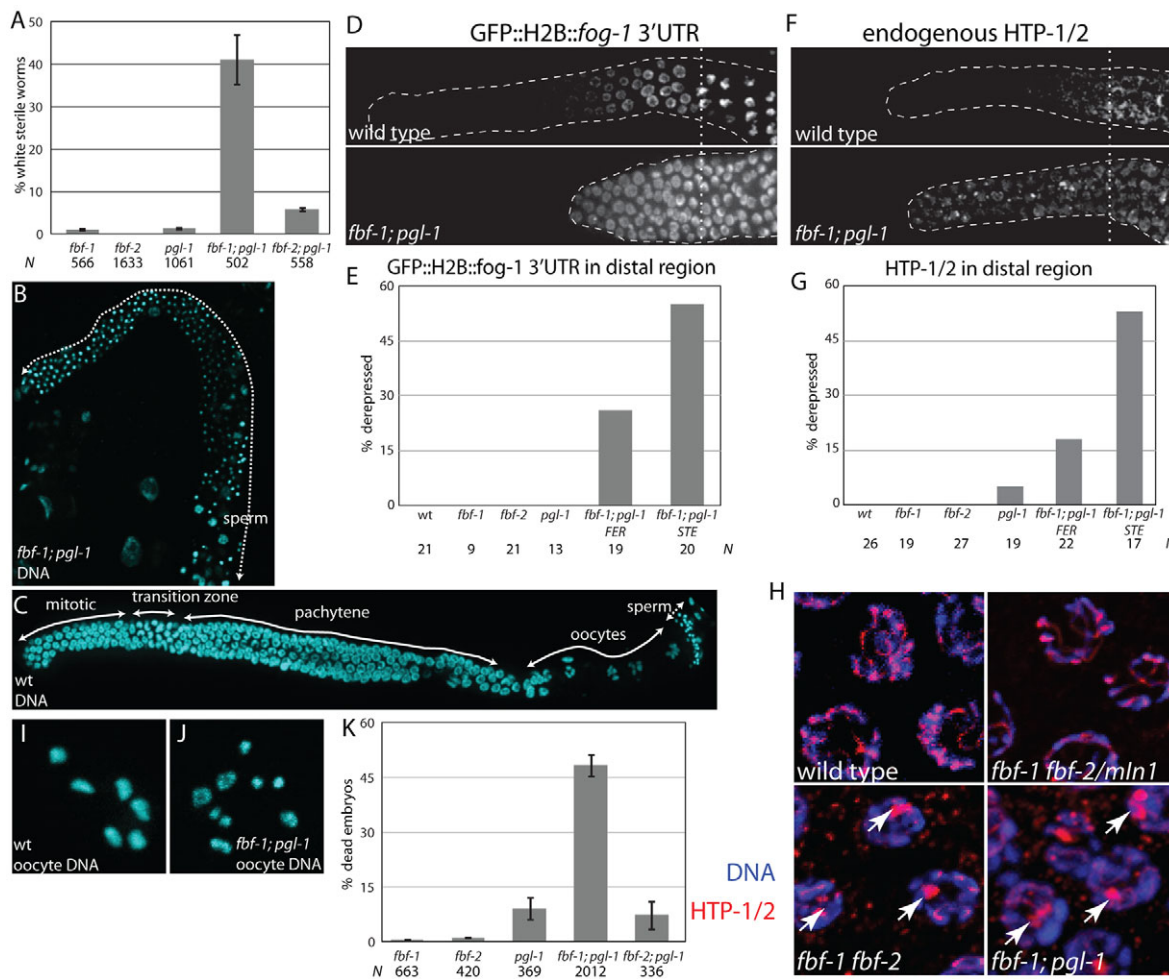
Fig. 3 *fbf-1;pgl-1* mutants show the same range of phenotypes as *fbf-1 fbf-2* mutants. (**A**) The percentage of sterile hermaphrodites of the indicated genotypes. Error bars indicate s.e.m. (from three to six experiments). *N*, number of hermaphrodites scored. (**B,C**) Full gonads of the indicated genotype stained with DAPI to reveal nuclei. The wild-type gonad contains all stages of germ cell differentiation including oocytes and sperm. By contrast, the *fbf-1;pgl-1* germline contains primarily spermatogenic cells (dotted line). Excess sperm was observed in 42% of *fbf-1;pgl-1* germlines. (**D,F**) Distal gonads of the indicated genotypes expressing a GFP::Histone H2B fusion under the control of the *fog-1* 3' UTR (D) or immunostained for the synaptonemal complex proteins HTP-1 and HTP-2 (F) [the antibody recognizes both proteins (Martinez-Perez et al., 2008)]. Gonads are outlined; vertical dotted lines indicate the position of the transition zone as recognized by the 'crescent-shaped' chromatin. (**E,G**) The percentage of gonads of the indicated genotypes with GFP::H2B:*fog-1* 3' UTR or HTP-1/2 expression extending to the distal end. *fbf-1;pgl-1* gonads are divided into two groups: those that were fertile (had embryos, *FER*) and those that were sterile (no embryos, *STE*). Gonads were scored at the young adult stage before all cells entered meiosis. A minority of gonads in which all cells had already entered meiosis (no mitotic zone) were excluded from analysis. (**H**) Magnified view of nuclei in the pachytene region stained for DNA (blue) and HTP-1/2 (red); maximum intensity projection of confocal stack spanning the depth of the nucleus. HTP-1/2 forms aggregates (arrows) in *fbf-1 fbf-2* and *fbf-1;pgl-1* double mutants, but not in wild-type or *fbf-1 fbf-2/mln1* (balancer) controls. (**I,J**) Magnified view of DAPI-stained chromosomes in diakinesis stage oocytes; maximum intensity projection of confocal stack spanning the depth of the nucleus. At this stage, homologous chromosomes should be held together by chiasmata forming six distinct DNA masses (wild type, I). Nine chromosomal masses are visible in an *fbf-1;pgl-1* oocyte (J) indicating that some homologs have failed to recombine. (**K**) The percentage of dead embryos produced by fertile hermaphrodites of the indicated genotypes. Error bars indicate s.e.m. (from two to seven experiments).

(*n*=140; Fig. 3J; supplementary material Fig. S3D) and 48% embryonic lethality (*n*=2012; Fig. 3K). We conclude that *fbf-1;pgl-1* mutants exhibit the same range of defects as *fbf-1 fbf-2* mutants, albeit with lower penetrance. These observations suggest that *pgl-1* is required for *fbf-2* activity.

FBF-1 and FBF-2 regulate different aspects of meiotic mRNA regulation

The finding that *pgl-1* is required primarily for *fbf-2* but not *fbf-1* activity suggests that, despite their sequence similarity, FBF-1 and

FBF-2 use different mechanisms to silence meiotic gene expression. To investigate this possibility further, we visualized meiotic mRNAs in *fbf-1*, *fbf-2* and *pgl-1* single- and double-mutant combinations using fluorescent in situ hybridization. We analyzed the FBF targets *gld-1*, *htp-1/2* and *him-3* and the non-FBF target *tbb-2*, which encodes β-tubulin, as a control. *tbb-2* mRNA was uniformly distributed throughout the distal region in all genotypes (Fig. 4; data not shown). As reported previously for *gld-1* (Jones et al., 1996), in wild-type gonads we detected low levels of *gld-1*, *htp-1/2* and *him-3* mRNAs in the distal half of the mitotic zone,

increasing levels in the proximal half of the mitotic zone, and high levels in the pachytene region (Fig. 4A). The same pattern was observed in *fbf-2* and *pgl-1* single mutants (Fig. 4A). By contrast, in *fbf-1* mutants we detected high levels of *gld-1*, *htp-1/2* and *him-3* mRNAs throughout the mitotic zone. In the mitotic zone, these mRNAs accumulated in several large aggregates that exceeded 1 μm in size (Fig. 4A,B). No such aggregates were observed with *tbb-2* mRNA (Fig. 4A,B). The RNA aggregates were reminiscent of the FBF-2 aggregates that also form in *fbf-1* mutants (Fig. 1E). Colocalization experiments confirmed that *gld-1* RNA and GFP::FBF-2 localize to the same aggregates in *fbf-1* mutants (Fig. 4C). The aggregates were dependent on both *fbf-2* and *pgl-1*: no, or fewer, RNA aggregates were observed in *fbf-1 fbf-2* or *fbf-1;pgl-1* double mutants (Fig. 4A,B). In those backgrounds, the mRNAs were uniformly distributed throughout the mitotic zone (Fig. 4A). We conclude that *fbf-1* functions to inhibit the accumulation of meiotic mRNAs in the distal half of the mitotic zone. *fbf-2* and *pgl-1* are not essential for this process, but are required for aggregation of the ectopic mRNAs that accumulate in *fbf-1* mutants. Examination of RNAs derived from transgenes under the control of the pan-germline promoter *pie-1* confirmed that these effects are post-transcriptional: GFP mRNA derived from the *pie-1* promoter:GFP::H2B *him-3* 3′ UTR reporter was distributed in a low-to-high gradient in the mitotic zone (supplementary material

Fig. S4A). By contrast, GFP mRNA derived from the same reporter but with mutations in the FBF-1/2 binding sites in the *him-3* 3′ UTR (Merritt and Seydoux, 2010) was distributed uniformly throughout the mitotic zone (supplementary material Fig. S4A).

The above findings suggest that silencing by FBF-1 involves post-transcriptional mechanisms that lower mRNA levels in the distal mitotic zone, whereas silencing by FBF-2 does not affect mRNA levels. If so, mRNA and protein levels should be correlated in *fbf-2* mutant gonads (where silencing depends on FBF-1), but not in *fbf-1* gonads (where silencing depends on FBF-2). To compare protein and RNA levels in the same gonads, we visualized *gld-1* RNA by situ hybridization in gonads expressing a *pie-1* promoter::GFP::H2B fusion under the control of the *gld-1* 3′ UTR (we could not detect GLD-1 protein directly because the in situ protocol is not compatible with immunofluorescence). We found that, as predicted, *gld-1* RNA and GFP levels correlated well throughout the mitotic zone in *fbf-2* mutant gonads, but not in wild-type or *fbf-1* gonads (supplementary material Fig. S4B). In the latter, significant levels of *gld-1* mRNA were detected in the distal end of the mitotic zone where GFP fluorescence was undetectable or low (supplementary material Fig. S4B). These observations confirm that silencing by FBF-2 primarily suppresses protein levels (mRNA translation), whereas silencing by FBF-1 also leads to a reduction (or redistribution) of mRNA levels.
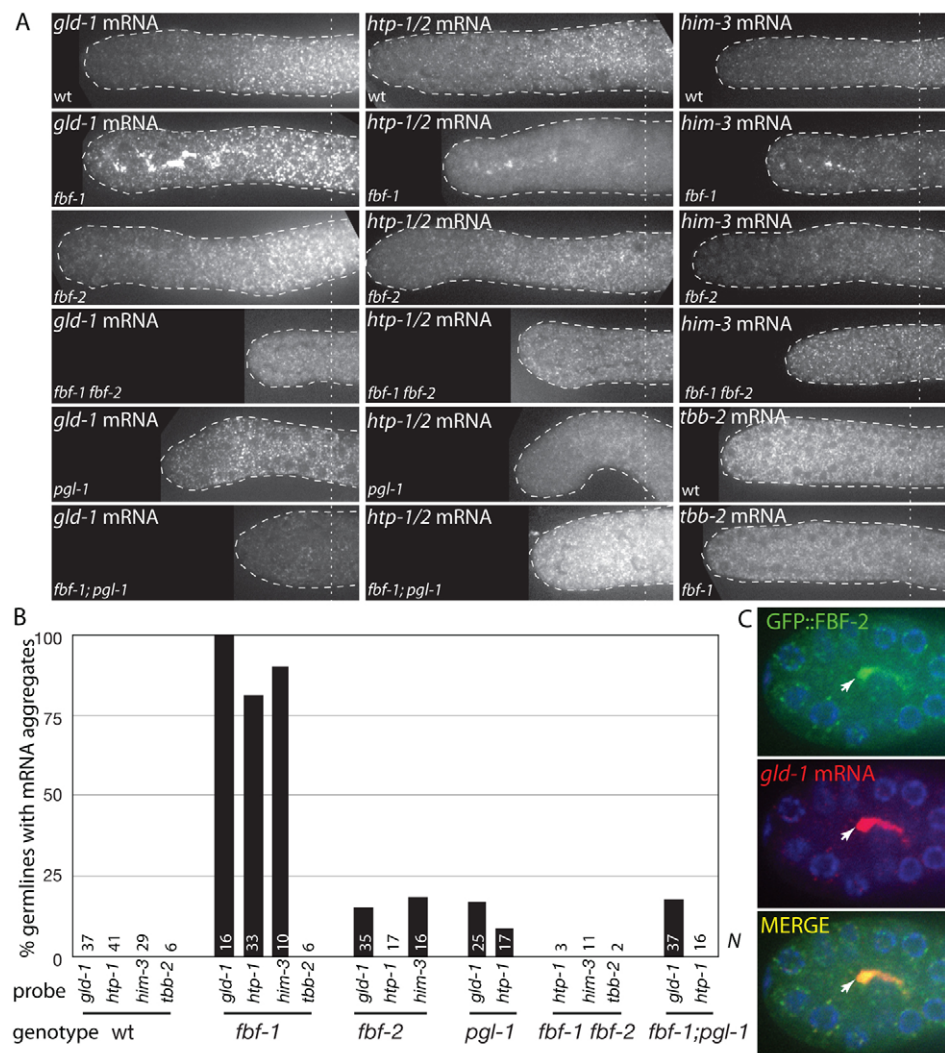
Fig. 4. *fbf-1* affects the distribution of meiotic mRNAs in the distal gonad. (**A**) Distal gonads of the indicated genotypes hybridized to fluorescent probes specific for *gld-1*, *htp-1/2*, *him-3* and *tbb-2* mRNAs. Germlines are outlined; vertical dotted lines indicate the transition zone as recognized by DAPI staining (not shown). (**B**) The percentage of germlines with aggregates of the indicated mRNAs as visualized by in situ hybridization as shown in A. *N*, the number of gonads scored for each genotype and mRNA. (**C**) *fbf-1* mutant distal gonad double stained for GFP::FBF-2 and *gld-1* mRNA. Arrow points to a cytoplasmic aggregate that is positive for both GFP::FBF-2 and *gld-1* mRNA.

PGL-1 is required for maximum binding of FBF-2 to target mRNAs

The observation that PGL-1 is required for the formation of FBF-2–mRNA aggregates in *fbf-1* mutants raised the possibility that PGL-1 promotes FBF-2 binding to target mRNAs. To test this hypothesis, we immunoprecipitated GFP::FBF-2 with an anti-GFP antibody (or with a control IgG) in lysates prepared from wild-type or *pgl-1* mutant worms and quantified the amounts of five known FBF-1/2 target mRNAs in the immunoprecipitates by qRT-PCR. Results were normalized for the amount of GFP::FBF-2 immunoprecipitated in three independent experiments and the amount of non-specific binding to the control IgG antibody (see Materials and methods). We found that target mRNAs were precipitated with higher efficiency from wild-type lysates than *pgl-1* lysates (Fig. 5A).

FBF-1 recognizes the same consensus sequence as FBF-2 in vitro (Bernstein et al., 2005) and co-immunoprecipitates at least some of the same RNAs (Merritt and Seydoux, 2010). We immunoprecipitated FBF-1 from the same wild-type and *pgl-1* lysates used for the GFP::FBF-2 immunoprecipitations, and observed no decrease in the ability of FBF-1 to interact with the target RNA *gld-1* (Fig. 5B). We observed a minor reduction in binding of FBF-1 to *htp-1*, *him-3* and *syp-3* mRNAs, but this decrease was observed in only one experimental replicate (data not shown) and was not statistically significant when averaged over all experimental replicates. We also examined the ability of a GLD-1::GFP fusion to interact with *gld-1* mRNA in wild-type and *pgl-1* lysates and again found no significant differences (Fig. 5C). We conclude that *pgl-1*

activity is required for maximal association of FBF-2 with target mRNAs, but is not essential for all protein-RNA interactions.

DISCUSSION

In this study we present evidence that FBF-1 and FBF-2 inhibit the expression of meiotic mRNAs in the distal germline by two distinct mechanisms and that PGL-1 is required for FBF-2 activity. We discuss each of these points in turn below.

FBF-1 and FBF-2 silence meiotic mRNAs by distinct mechanisms

In situ hybridization experiments on fixed adult gonads revealed that the *gld-1*, *htp-1/2* and *him-3* mRNAs are distributed in a gradient in the mitotic zone, with the lowest signal at the distal end (where the stem cells reside) and the highest signal toward the proximal end (transition zone, where meiosis starts). This pattern does not depend on FBF-2 or PGL-1: *fbf-2* and *pgl-1* mutants maintain a distal-low/proximal-high gradient of meiotic RNAs. By contrast, in *fbf-1* mutants, meiotic mRNAs accumulate in several aggregates throughout the rachis of the mitotic zone, including at the distal end. Because all cells are connected to a central core that runs through the mitotic zone and into the pachytene region (Hubbard and Greenstein, 2005), we do not know whether FBF-1 'clears' meiotic mRNAs from the distal end by promoting their degradation or transport. In the proximal germline, cytoplasmic streaming transports mitochondria and small PGL-1::GFP particles from the pachytene region into oocytes (Wolke et al., 2007). No
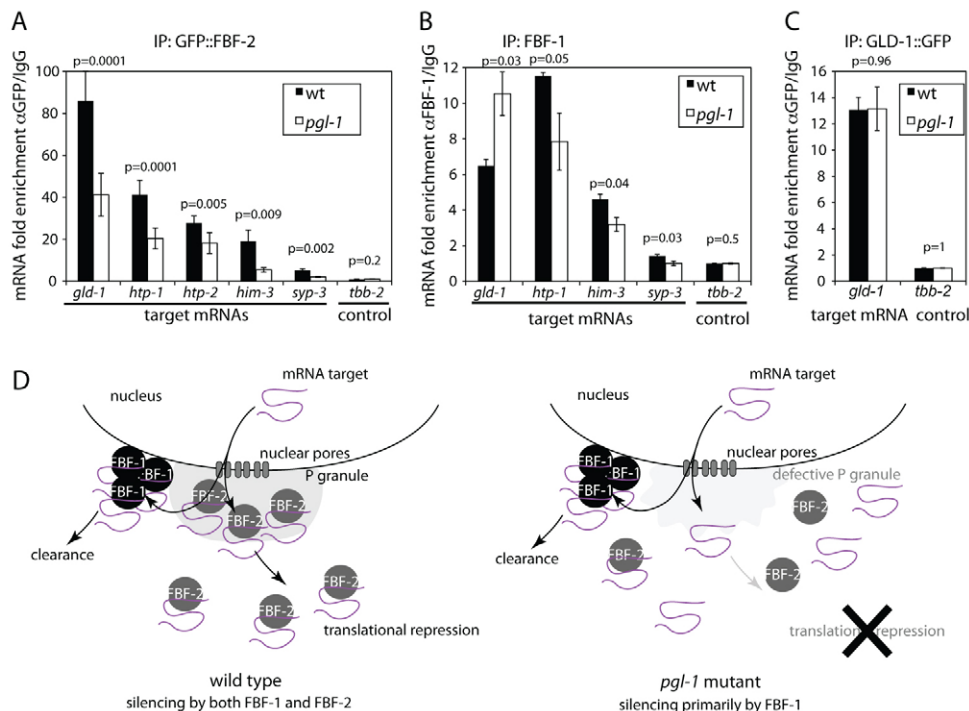
Fig. 5. Efficient immunoprecipitation of meiotic mRNAs by GFP::FBF-2 requires *pgl-1*. (**A-C**) Enrichment of the indicated mRNAs in immunoprecipitates of GFP::FBF-2, FBF-1 and GLD-1::GFP in wild-type and *pgl-1* extracts as determined by qPCR. The mean is calculated from two (FBF-1) or three (GFP::FBF-2, GLD-1::GFP) biological replicates. Error bars indicate s.e.m. *P*-values evaluating difference between wild type and *pgl-1* are shown for each analyzed mRNA. Western blots used to equalize cDNA loading per amount of precipitated protein are shown in supplementary material Fig. S5A-C. Levels of analyzed mRNAs in the input lysates normalized to *ama-1* mRNA are shown in supplementary material Fig. S5D. (**D**) Working model of cooperation between FBF-2 and PGL-1. In the mitotic zone, upon exit from the nucleus, mRNAs encoding meiotic proteins encounter FBF-2 in P granules or FBF-1 in other perinuclear granules. mRNAs bound by FBF-2 are maintained in the cytoplasm in translationally repressed complexes. mRNAs bound by FBF-1 are cleared from the cytoplasm by an unknown mechanism. In *pgl-1* mutants, FBF-2 fails to localize to P granules and does not bind efficiently to its target mRNAs. FBF-1 is unaffected.

such bulk movement, however, has been observed in the mitotic zone. If FBF-1 promotes mRNA transport, it must do so by targeting specific mRNAs, as tubulin mRNA was not in a gradient and the graded distribution of the *him-3* 3′ UTR reporter mRNA was dependent on FBF-1/2 binding sites.

Expression of GLD-1 and of the meiotic 3′ UTR reporters is partially derepressed in the mitotic zone of *fbf-1* mutants and completely derepressed in *fbf-1 fbf-2* mutants (Crittenden et al., 2002; Suh et al., 2009; Merritt and Seydoux, 2010). Thus, in the absence of FBF-1, FBF-2 incompletely suppresses the translation of meiotic mRNAs in the distal region. This suppression correlates with the formation of aggregates that contain both FBF-2 and meiotic mRNAs: the aggregates are observed in *fbf-1* mutants but not in *fbf-1 fbf-2* and *fbf-1;pgl-1* double mutants, in which the meiotic mRNAs are no longer silenced. We suggest that the aggregates represent translationally repressed FBF-2–mRNA complexes, which in wild-type gonads are degraded or transported out of the region by FBF-1. Consistent with this hypothesis, as is true for meiotic mRNAs, FBF-2 levels are lowest in the five distalmost rows and this pattern depends on FBF-1 (Fig. 1E).

Our findings indicate that despite their sequence similarity and shared binding sites, FBF-1 and FBF-2 have different effects on the distribution of meiotic mRNAs. One possibility is that binding by either FBF-1 or FBF-2 blocks translation, and binding by FBF-1 additionally leads to RNA degradation or transport. In vitro, both FBF-1 and FBF-2 bind the Pop2 subunit of the CCR4-Pop2-NOT deadenylation complex, and FBF-2 can stimulate deadenylation by the yeast Pop2 complex (Suh et al., 2009). Shortening of the poly(A) tail could in principle lead to both translation inhibition and RNA degradation (Goldstrohm et al., 2006; Hook et al., 2007). Loss of Pop2 activity moderately increases GLD-1 levels in the distal gonad, confirming that deadenylation is one of the mechanisms used by the FBFs to silence mRNAs, but not the only one (Suh et al., 2009). Recently, FBF-1 has also been shown to inhibit the GTPase activity of elongation factor eIF1A in a complex with the Argonaute protein CSR-1. In vitro, the FBF-1–CSR-1–eIF1A complex stalls ribosomes during elongation (Friend et al., 2012). Interestingly, in yeast, translational repression by PUF proteins has been linked to localization of the silenced mRNA to distinct subcellular regions. Puf6 promotes the assembly of 'locasome complexes' on the *ASH1* mRNA by relieving the competition between ribosomes and the localization factor She2 (Gu et al., 2004; Deng et al., 2008). Binding by She2 in turn localizes *ASH1* mRNA to the daughter bud. Similarly, Puf5 promotes the localization of the *Pex14* mRNA to peroxisomes, and Puf3 localizes its many mRNA targets to mitochondria (reviewed by Quenault et al., 2011).

We suggest that, like other PUFs, FBF-1 and FBF-2 have diverged enough to interact with different factors. FBF-1 and FBF-2 are 95% identical throughout their RNA-binding domain, but only show 87% and 72% identity in their N- and C-termini, respectively. These divergent domains might provide interaction surfaces for distinct co-factors leading to different modes of RNA regulation. Consistent with interacting with different protein partners, FBF-1 and FBF-2 accumulate in different cytoplasmic granules. FBF-1 localizes to many unidentified granules throughout the cytoplasm, whereas FBF-2 localizes primarily to P granules around nuclei and is more diffusely distributed in the cytoplasm. Because FBF-1 and FBF-2 recognize the same sequence, one possibility is that they compete for targets. We suggest that, in the distal end of the mitotic zone, an unknown mechanism, possibly dependent on Notch signaling from the distal tip cell (Kimble,

2011), suppresses FBF-2 activity and/or levels, allowing FBF-1 to clear meiotic mRNAs from this region. In more proximal rows, FBF-2 competes effectively with FBF-1, causing meiotic mRNAs to accumulate while remaining translationally repressed. Competition between FBF-1 and FBF-2 could also explain why the mutants have opposite effects on the size of the mitotic zone (Lamont et al., 2004). In the absence of FBF-1, meiotic mRNAs accumulate throughout the mitotic zone, leading to premature meiotic entry (shorter mitotic zone). In *fbf-2* mutants, FBF-1 keeps meiotic mRNA levels low, delaying meiotic entry (longer mitotic zone). It will be interesting to investigate what keeps FBF-2 activity/levels low in the distalmost mitotic zone: FBF-1 is required, but cannot be the only factor because FBF-1 is also present in the proximal half of the mitotic zone where FBF-2 levels are high (Fig. 1).

PGL-1 contributes to FBF-2-dependent silencing

Several lines of evidence indicate that PGL-1 functions with FBF-2 to promote the silencing of meiotic mRNAs. Both *fbf-2* and *pgl-1* mutants are fertile on their own but become sterile when combined with mutations in *fbf-1*. *fbf-1;pgl-1* mutants share several phenotypes with *fbf-1 fbf-2* mutants, including sterility, excess sperm, derepression of meiotic mRNAs in the mitotic zone, defective loading of the synaptonemal complex during meiosis, and defects in meiotic recombination. These defects are less penetrant in *fbf-1;pgl-1* mutants than in *fbf-1 fbf-2* mutants, suggesting that *pgl-1* is only partially required for *fbf-2* activity, perhaps because of redundancy with other P granule components. Consistent with these findings, FBF-2 binding to target RNAs is reduced, but not completely eliminated, in extracts from *pgl-1* mutants. FBF-2 is enriched on P granules and this enrichment is lost in *pgl-1* mutants. FBF-2 activity and localization to P granules are also compromised in *glh-1(RNAi)* gonads, where PGL-1 is present but no longer on P granules. These findings suggest that localization to P granules, rather than PGL-1 function per se, is necessary to maximize FBF-2 activity.

P granules are major sites of RNA export from the nucleus (Sheth et al., 2010) and have been proposed to extend the nuclear pore environment into the cytoplasm (Updike et al., 2011). Like nuclear pores, P granules establish a size-exclusion barrier (Updike et al., 2011). Such a barrier could create a privileged environment in which mRNAs are able to interact with regulators such as FBF-2 without interference from ribosomes or other translation-promoting factors. The assembly of multivalent complexes in P granules could also greatly increase the local concentration of RNA-binding proteins (Li et al., 2012). As most RNAs do not appear to accumulate in P granules upon exit from the nucleus (Sheth et al., 2010), we suggest that meiotic mRNAs meet FBF-2 while transiting through the P granules and enter the cytoplasm complexed with FBF-2 in a silenced mRNP (Fig. 5D). Consistent with this hypothesis, in *fbf-1* mutants, we observed large FBF-2–meiotic mRNA aggregates in the cytoplasm away from P granules, and formation of these aggregates was dependent on *pgl-1*.

A role for P granules in mRNA regulation has been suggested ever since their discovery as RNA-rich structures (reviewed by Voronina et al., 2011; Schisa, 2012). Our data demonstrate that PGL-1 facilitates translational silencing by FBF-2, but this is unlikely to be the only role of PGL-1. *pgl-1* mutants display several phenotypes not seen in *fbf-2* mutants, including resistance to RNAi (Robert et al., 2005; Spike et al., 2008b), a short mitotic zone (supplementary material Fig. S3B) and sterility at 25°C (Kawasaki et al., 1998). PGL-1 is a key structural component of P granules: PGL-1 is

required (with its homolog PGL-3) for P granule formation in embryos and can form ectopic granules when expressed in somatic cells (Hanazawa et al., 2011; Updike et al., 2011). It will be interesting to determine which RNA-binding proteins besides FBF-2 require PGL-1 to function efficiently in germ cells.

Competing interests statement
The authors declare no competing financial interests.

Supplementary material
Supplementary material available online at
http://dev.biologists.org/lookup/suppl/doi:10.1242/dev.083980/-/DC1

References
Arur, S., Ohmachi, M., Nayak, S., Hayes, M., Miranda, A., Hay, A., Golden, A. and Schedl, T. (2009). Multiple ERK substrates execute single biological processes in Caenorhabditis elegans germ-line development. *Proc. Natl. Acad. Sci. USA* **106**, 4776-4781.

Bernstein, D., Hook, B., Hajarnavis, A., Opperman, L. and Wickens, M. (2005). Binding specificity and mRNA targets of a C. elegans PUF protein, FBF-1. *RNA* **11**, 447-458.

Brenner, S. (1974). The genetics of Caenorhabditis elegans. *Genetics* **77**, 71-94.

Cinquin, O., Crittenden, S. L., Morgan, D. E. and Kimble, J. (2010). Progression from a stem cell-like state to early differentiation in the C. elegans germ line. *Proc. Natl. Acad. Sci. USA* **107**, 2048-2053.

Crittenden, S. L., Bernstein, D. S., Bachorik, J. L., Thompson, B. E., Gallegos, M., Petcherski, A. G., Moulder, G., Barstead, R., Wickens, M. and Kimble, J. (2002). A conserved RNA-binding protein controls germline stem cells in Caenorhabditis elegans. *Nature* **417**, 660-663.

Deng, Y., Singer, R. H. and Gu, W. (2008). Translation of ASH1 mRNA is repressed by Puf6p-Fun12p/eIF5B interaction and released by CK2 phosphorylation. *Genes Dev.* **22**, 1037-1050.

Friend, K., Campbell, Z. T., Cooke, A., Kroll-Conner, P., Wickens, M. P. and Kimble, J. (2012). A conserved PUF-Ago-eEF1A complex attenuates translation elongation. *Nat. Struct. Mol. Biol.* **19**, 176-183.

Goldstrohm, A. C., Hook, B. A., Seay, D. J. and Wickens, M. (2006). PUF proteins bind Pop2p to regulate messenger RNAs. *Nat. Struct. Mol. Biol.* **13**, 533-539.

Gruidl, M. E., Smith, P. A., Kuznicki, K. A., McCrone, J. S., Kirchner, J., Roussell, D. L., Strome, S. and Bennett, K. L. (1996). Multiple potential germ-line helicases are components of the germ-line-specific P granules of Caenorhabditis elegans. *Proc. Natl. Acad. Sci. USA* **93**, 13837-13842.

Gu, W., Deng, Y., Zenklusen, D. and Singer, R. H. (2004). A new yeast PUF family protein, Puf6p, represses ASH1 mRNA translation and is required for its localization. *Genes Dev.* **18**, 1452-1465.

Hanazawa, M., Yonetani, M. and Sugimoto, A. (2011). PGL proteins self associate and bind RNPs to mediate germ granule assembly in C. elegans. *J. Cell Biol.* **192**, 929-937.

Hansen, D., Wilson-Berry, L., Dang, T. and Schedl, T. (2004). Control of the proliferation versus meiotic development decision in the C. elegans germline through regulation of GLD-1 protein accumulation. *Development* **131**, 93-104.

Hook, B. A., Goldstrohm, A. C., Seay, D. J. and Wickens, M. (2007). Two yeast PUF proteins negatively regulate a single mRNA. *J. Biol. Chem.* **282**, 15430-15438.

Hubbard, E. J. A. and Greenstein, D. (2005). Introduction to the germ line. *WormBook* 1-4, www.wormbook.org.

Jones, A. R., Francis, R. and Schedl, T. (1996). GLD-1, a cytoplasmic protein essential for oocyte differentiation, shows stage- and sex-specific expression during Caenorhabditis elegans germline development. *Dev. Biol.* **180**, 165-183.

Kamath, R. S. and Ahringer, J. (2003). Genome-wide RNAi screening in Caenorhabditis elegans. *Methods* **30**, 313-321.

Kawasaki, I., Shim, Y. H., Kirchner, J., Kaminker, J., Wood, W. B. and Strome, S. (1998). PGL-1, a predicted RNA-binding component of germ granules, is essential for fertility in C. elegans. *Cell* **94**, 635-645.

Kershner, A. M. and Kimble, J. (2010). Genome-wide analysis of mRNA targets for Caenorhabditis elegans FBF, a conserved stem cell regulator. *Proc. Natl. Acad. Sci. USA* **107**, 3936-3941.

Kimble, J. (2011). Molecular regulation of the mitosis/meiosis decision in multicellular organisms. *Cold Spring Harb. Perspect. Biol.* **3**, a002683.

Lamont, L. B., Crittenden, S. L., Bernstein, D., Wickens, M. and Kimble, J. (2004). FBF-1 and FBF-2 regulate the size of the mitotic region in the C. elegans germline. *Dev. Cell* **7**, 697-707.

Lee, M. H., Hook, B., Pan, G., Kershner, A. M., Merritt, C., Seydoux, G., Thomson, J. A., Wickens, M. and Kimble, J. (2007). Conserved regulation of MAP kinase expression by PUF RNA-binding proteins. *PLoS Genet.* **3**, e233.

Li, P., Banjade, S., Cheng, H. C., Kim, S., Chen, B., Guo, L., Llaguno, P., Hollingsworth, J. V., King, D. S., Banani, S. F. et al. (2012). Phase transitions in the assembly of multivalent signalling proteins. *Nature* **483**, 336-340.

Luitjens, C., Gallegos, M., Kraemer, B., Kimble, J. and Wickens, M. (2000). CPEB proteins control two key steps in spermatogenesis in C. elegans. *Genes Dev.* **14**, 2596-2609.

Martinez-Perez, E., Schvarzstein, M., Barroso, C., Lightfoot, J., Dernburg, A. F. and Villeneuve, A. M. (2008). Crossovers trigger a remodeling of meiotic chromosome axis composition that is linked to two-step loss of sister chromatid cohesion. *Genes Dev.* **22**, 2886-2901.

Merritt, C. and Seydoux, G. (2010). The Puf RNA-binding proteins FBF-1 and FBF-2 inhibit the expression of synaptonemal complex proteins in germline stem cells. *Development* **137**, 1787-1798.

Merritt, C., Rasoloson, D., Ko, D. and Seydoux, G. (2008). 3′ UTRs are the primary regulators of gene expression in the C. elegans germline. *Curr. Biol.* **18**, 1476-1482.

Pitt, J. N., Schisa, J. A. and Priess, J. R. (2000). P granules in the germ cells of Caenorhabditis elegans adults are associated with clusters of nuclear pores and contain RNA. *Dev. Biol.* **219**, 315-333.

Praitis, V., Casey, E., Collar, D. and Austin, J. (2001). Creation of low-copy integrated transgenic lines in Caenorhabditis elegans. *Genetics* **157**, 1217-1226.

Qiu, C., Kershner, A., Wang, Y., Holley, C. P., Wilinski, D., Keles, S., Kimble, J., Wickens, M. and Hall, T. M. (2012). Divergence of Pumilio/fem-3 mRNA binding factor (PUF) protein specificity through variations in an RNA-binding pocket. *J. Biol. Chem.* **287**, 6949-6957.

Quenault, T., Lithgow, T. and Traven, A. (2011). PUF proteins: repression, activation and mRNA localization. *Trends Cell Biol.* **21**, 104-112.

Raj, A., van den Bogaard, P., Rifkin, S. A., van Oudenaarden, A. and Tyagi, S. (2008). Imaging individual mRNA molecules using multiple singly labeled probes. *Nat. Methods* **5**, 877-879.

Rangan, P., DeGennaro, M. and Lehmann, R. (2008). Regulating gene expression in the Drosophila germ line. *Cold Spring Harb. Symp. Quant. Biol.* **73**, 1-8.

Robert, V. J., Sijen, T., van Wolfswinkel, J. and Plasterk, R. H. (2005). Chromatin and RNAi factors protect the C. elegans germline against repetitive sequences. *Genes Dev.* **19**, 782-787.

Schisa, J. (2012). New insights into the regulation of RNP granule assembly in oocytes. *Int. Rev. Cell Mol. Biol.* **295**, 233-289.

Sheth, U., Pitt, J., Dennis, S. and Priess, J. R. (2010). Perinuclear P granules are the principal sites of mRNA export in adult C. elegans germ cells. *Development* **137**, 1305-1314.

Spike, C., Meyer, N., Racen, E., Orsborn, A., Kirchner, J., Kuznicki, K., Yee, C., Bennett, K. and Strome, S. (2008a). Genetic analysis of the Caenorhabditis elegans GLH family of P-granule proteins. *Genetics* **178**, 1973-1987.

Spike, C. A., Bader, J., Reinke, V. and Strome, S. (2008b). DEPS-1 promotes P-granule assembly and RNA interference in C. elegans germ cells. *Development* **135**, 983-993.

Suh, N., Crittenden, S. L., Goldstrohm, A., Hook, B., Thompson, B., Wickens, M. and Kimble, J. (2009). FBF and its dual control of gld-1 expression in the Caenorhabditis elegans germline. *Genetics* **181**, 1249-1260.

Thompson, B. E., Bernstein, D. S., Bachorik, J. L., Petcherski, A. G., Wickens, M. and Kimble, J. (2005). Dose-dependent control of proliferation and sperm specification by FOG-1/CPEB. *Development* **132**, 3471-3481.

Timmons, L. and Fire, A. (1998). Specific interference by ingested dsRNA. *Nature* **395**, 854.

Updike, D. and Strome, S. (2010). P granule assembly and function in Caenorhabditis elegans germ cells. *J. Androl.* **31**, 53-60.

Updike, D. L., Hachey, S. J., Kreher, J. and Strome, S. (2011). P granules extend the nuclear pore complex environment in the C. elegans germ line. *J. Cell Biol.* **192**, 939-948.

Voronina, E. and Seydoux, G. (2010). The C. elegans homolog of nucleoporin Nup98 is required for the integrity and function of germline P granules. *Development* **137**, 1441-1450.

Voronina, E., Seydoux, G., Sassone-Corsi, P. and Nagamori, I. (2011). RNA granules in germ cells. *Cold Spring Harb. Perspect. Biol.* **3**, pii: a002774.

Wolke, U., Jezuit, E. A. and Priess, J. R. (2007). Actin-dependent cytoplasmic streaming in C. elegans oogenesis. *Development* **134**, 2227-2236.